Cerebral Cortex, November 2019; 4646–4653

doi: 10.1093/cercor/bhy342
Advance Access Publication Date: 21 January 2019
Original Article

ORIGINAL ARTICLE

Biological Characteristics of Connection-Wise Resting-State Functional Connectivity Strength

Rory Pijnenburg [1], Lianne H. Scholtens [1], Dante Mantini [2,3], Wim Vanduffel[4,5,6], Lisa Feldman Barrett[6,7] and Martijn P. van den Heuvel[1,8]

[1]Connectome Lab, Department of Complex Trait Genetics, Center for Neurogenomics and Cognitive Research, Faculty of Science, Vrije Universiteit Amsterdam, Amsterdam Neuroscience, De Boelelaan 1081-1087, 1081 HV Amsterdam, The Netherlands, [2]Research Center for Motor Control and Neuroplasticity, KU Leuven, Tervuursevest 101 - box 1501 - 3001 Leuven, Belgium, [3]Functional Neuroimaging Laboratory, IRCCS San Camillo Hospital Foundation, Via Alberoni, 70, 30126 Lido VE, Italy, [4]Laboratory for Neuro- and Psychophysiology, O&N II Herestraat 49 - box 1021 3000 Leuven, Belgium, [5]Department of Radiology, Harvard Medical School, Massachusetts General Hospital, Radiology/NMR Ctr - 2nd FL 149 13th Street, Charlestown MA 02129, USA, [6]Department of Psychiatry and Athinoula A. Martinos Center for Biomedical Imaging, Massachusetts General Hospital, 149 Thirteenth Street, Suite 2301, Charlestown, MA 02129, USA, [7]Department of Psychology, Northeastern University, 125 NI (Nightingale Hall), Boston, MA 02115, USA and [8]Department of Clinical Genetics, VU University Medical Center, Amsterdam Neuroscience, De Boelelaan 1117, 1081 HV Amsterdam, The Netherlands

Address correspondence to Martijn van den Heuvel, Connectome Lab, Department of Complex Trait Genetics, Faculty of Science, Center for Neurogenomics and Cognitive Research, Vrije Universiteit Amsterdam, Amsterdam Neuroscience, Room B-651, De Boelelaan 1081-1087, 1081 HV Amsterdam, The Netherlands. Email: martijn.vanden.heuvel@vu.nl

Abstract

Functional connectivity is defined as the statistical dependency of neurophysiological activity between 2 separate brain areas. To investigate the biological characteristics of resting-state functional connectivity (rsFC)—and in particular the significance of connection-wise variation in time-series correlations—rsFC was compared with strychnine-based connectivity measured in the macaque. Strychnine neuronography is a historical technique that induces activity in cortical areas through means of local administration of the substance strychnine. Strychnine causes local disinhibition through GABA suppression and leads to subsequent activation of functional pathways. Multiple resting-state fMRI recordings were acquired in 4 macaques (examining in total 299 imaging runs) from which a group-averaged rsFC matrix was constructed. rsFC was observed to be higher ($P < 0.0001$) between region-pairs with a strychnine-based connection as compared with region-pairs with no strychnine-based connection present. In particular, higher resting-state connectivity was observed in connections that were relatively stronger (weak < moderate < strong; $P < 0.01$) and in connections that were bidirectional ($P < 0.0001$) instead of unidirectional in strychnine-based connectivity. Our results imply that the level of correlation between brain areas as extracted from resting-state fMRI relates to the strength of underlying interregional functional pathways.

Key words: correlation, functional connectivity, resting-state, strength, strychnine

Introduction

The cerebrum of the mammalian brain consists of a large number of spatially separate and specialized areas which are structurally and functionally interconnected (Bullmore and Sporns 2009; Yeo et al. 2011). Communication between cortical areas is often examined by means of functional connectivity, defined as the statistical dependency of neurophysiological activity between separate brain regions (Friston 2011). Functional connectivity is an important tool to study brain organization and is often examined by means of resting-state functional magnetic resonance imaging (rs-fMRI). Using functional connectivity, a nonuniform distribution of connections across the brain was observed (Buckner and Vincent 2007; Buckner et al. 2009; Grayson et al. 2014), combined with the existence of multiple functional subnetworks (Damoiseaux et al. 2006; Yeo et al. 2011). Moreover, changes in functional connectivity are associated with several brain pathologies (Tian et al. 2006; Greicius 2008; Keown et al. 2017) and variation in behavior (Yuan et al. 2016; Balan et al. 2017). Properties of anatomical connections such as the projection distance, spatial location and number of white matter pathways have been associated with functional connectivity strength (Hermundstad et al. 2013). Anatomical connectivity as derived from tract tracing and diffusion tensor imaging have thus been suggested to underlie interregional functional connectivity (Kötter and Sommer 2000; Van den Heuvel et al. 2008; Damoiseaux and Greicius 2009; Honey et al. 2009). The interpretability of functional connectivity strength remains however complex due to an incomplete understanding of the underlying biological characteristics of the resting-state functional connectivity (rsFC) signal (Logothetis 2003; Friston 2011). One of the aspects that remains open is whether variation in the extracted fMRI connection-wise correlation values is related to the strength of underlying functional pathways. Here we studied resting-state functional correlations by comparing rsFC with information on the biological presence, strength and directionality of strychnine-based connectivity.

Strychnine neuronography is a classical technique first employed by Dusser de Barenne and McCulloch around a 100 years ago. Their studies were among the first systematic studies on brain connectivity in the mammalian brain (Fig. 1A; Dusser de Barenne 1916; Dusser de Barenne and McCulloch 1938; Dusser de Barenne et al. 1938). In their experiments, large parts of the macaque cerebral cortex were systematically tested for the propagation of locally induced activity by the administration of strychnine directly onto the surface of a cortical area (Stephan et al. 2000). Data that was later collated by Stephan and colleagues into a strychnine-based connectivity matrix (Fig. 1B; Stephan et al. 2000). In this study, we combined strychnine-based functional connectivity (stryFC) with modern-day measurements of rsFC. We show that the correlation strength of rsFC is related to the presence, directionality and in particular the strength of stryFC pathways.

Methods

Strychnine Neuronography

Strychnine neuronography connectivity data was adopted from the study of Stephan et al. (2000) who collated 19 studies of Dusser de Barenne and McCulloch among others (Dusser de Barenne 1916; Dusser de Barenne and McCulloch 1938), combining in total 3897 in vivo strychninization experiments in the macaque cortex (Stephan et al. 2000). The methodology employed in the strychnine neuronography studies remained as originally developed by Dusser de Barenne (Dusser de Barenne and McCulloch 1938; Stephan et al. 2000). The 3% strychnine solution used, was dyed with toluidine blue to visualize the strychninized surface of the cortex. Approximately 1 to a maximum of 4 mm^2 of cortex was included per strychninization experiment (Dusser de Barenne 1916). The activation patterns observed using strychnine neuronography were shown to be similar to the connectivity patterns after electrical stimulation of the same patch of cortex (Dusser de Barenne and McCulloch 1938; Dusser de Barenne et al. 1938; Bailey et al.

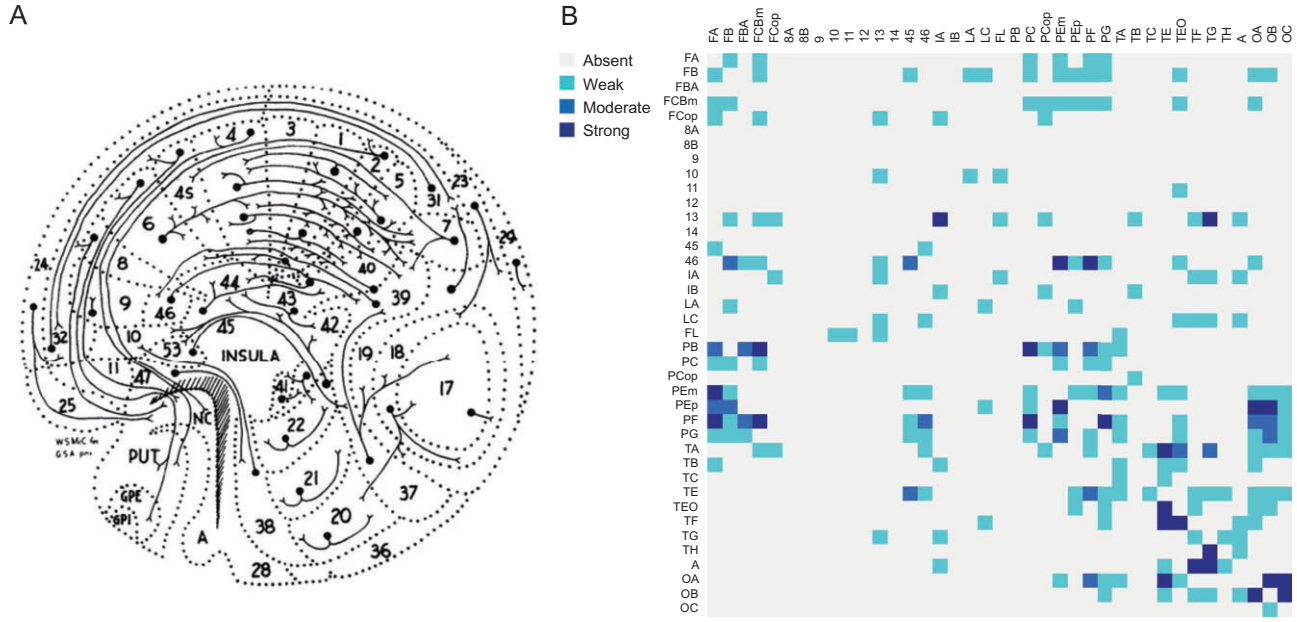

Figure 1. Strychnine neuronography. (*A*) Graphical representation of corticocortical and corticostriatal connections of the macaque cortex as observed with strychnine neuronography (McCulloch 1944). (*B*) The strychnine-based functional connectivity matrix of the macaque, containing absent/unreported connections (gray), weak/unknown strength (light blue), moderate (blue) and strong (dark blue) connections as measured by strychnine neuronography and collated by Stephan et al. (2000).

1944; Chusid et al. 1948; French et al. 1948). Robustness of this technique was further substantiated by the observation that the measurements were electrophysiological and spatially reproducible within the same animal and per area across animals (Dusser de Barenne and McCulloch 1938; Dusser de Barenne et al. 1938).

Strychnine acts as a partial antagonist for cortical inhibitory γ-aminobutyric acid-α ($GABA_A$) and as an antagonist for glycine receptors (GlyR) (Shirasaki et al. 1991; Takahashi et al. 1994). The application of strychnine therefore caused a (partial and reversible) temporal discontinuation of inhibitory postsynaptic potentials (Davidoff et al. 1969; Curtis et al. 1971). Strychnine induced disinhibition led to a locally increased neuronal firing rate and signal propagation along the efferent pathways of the strychninized area (Dusser de Barenne and McCulloch 1938). A distinct cortical activation pattern was revealed for each separately strychninized source area.

Dusser de Barenne (1916) further described that they could not observe motor symptoms (e.g., twitchings, hyper-reflexia) in response to strychninization of the motor cortex. They stated that this may have been due to the slight application of strychnine which was probably confined to the more superficial layers of the cortex, with motor neurons (Betz cells) located in deeper layers (Dusser de Barenne 1916; Kiernan and Hudson 1991). Moreover, experiments of isolation of the whole sensory cortex (as the connectivity profile was measured within this group of brain regions) by deep undercutting (i.e., cutting through all white matter connections) did not change strychnine-induced activity patterns (Dusser de Barenne and McCulloch 1938). It was thus concluded that the strychnine-induced activity was facilitated by corticocortical association fibers and not by corticosubcortical fibers (Dusser de Barenne and McCulloch 1938).

In the original strychninization experiments, signal propagation between cortical areas was measured using electrocorticography (ECoG). The strength of every connection was classified by Stephan et al. (2000) into different categories based on the amplitude of the ECoG signal in the target area. The strychnine neuronography results were then mapped onto a 39-by-39 Walker-Von Bonin & Bailey 1947 (WBB47) connectivity matrix by Objective Relational Transformation (Stephan et al. 2000). More details on the parcellation atlas used in this study can be found in Figure S1 and Table S1 in the Supplemental Information. The resulting matrix consists of connections between region pairs represented as "0" (absent, no connection, $n = 428$), "1" (present, weak connection strength, $n = 51$), "2" (present, moderate connection strength, $n = 20$), "3" (present, strong connection strength, $n = 26$), "4" (present, unknown connection strength, $n = 124$), or "-" ($n = 833$) where no information on a corticocortical connection was described (Stephan et al. 2000). All data on both hemispheres were pooled and combined into one unihemispheric connectivity matrix (Fig. 1B; Stephan et al. 2000). Binary strychnine connectivity data (describing the absence/presence of connections) was used in the analysis on the presence of connections, as well as in the analysis on the directionality of connections. The weighted version of this strychnine-based connectome, including information on the strength of strychnine connections, was used for the evaluation of the strength of resting-state functional connections.

Resting-State fMRI Functional Connectivity

Cortical functional connectivity was derived from 327 resting-state fMRI recordings, divided over 5–6 scanning sessions of 4 macaques (3 males, 1 female), as acquired in previous studies (Mantini et al. 2011, 2013). The awake animals were trained in a mock MRI scanner to fixate on a red dot that was centered upon a blank screen (Vanduffel et al. 2001). Upon reaching a 95% fixation rate, the monkeys were placed in a 3 T MR Siemens Trio scanner after which each individual completed either 5 (1 animal) or 6 (3 animals) resting-state scans with a duration of 10 min (all scans were acquired over a period of 6 months). A gradient-echo T2-weighted echo-planar sequence was used to obtain the functional images (40 slices, 84-by-84 in-plane matrix, repetition time (TR) = 2000 ms, echo time (TE) = 19 ms, flip angle = 75°, voxel size = 1.25 mm by 1.25 mm by 1.25 mm, 300 volumes per run). Each separate scan consisted of 14 resting-state fMRI runs on average (minimum 7, maximum 24 runs per session), which led to a total of 327 imaging runs. Accompanying T1-weighted anatomical images were obtained during different sessions using a magnetization-prepared rapid gradient echo (MP-RAGE) sequence (TR = 2200 ms, TE = 4.06 ms, voxel size = 0.5 mm by 0.5 mm by 0.5 mm). During the anatomical scans, the animals were sedated using ketamine/xylazine (ketamine 10 mg/kg I.M. 1 xylazine 0.5 mg/kg I.M., maintenance dose of 0.01–0.05 mg ketamine per minute I.V.). Preprocessing of the data was performed using SPM8.0 software (http://www.fil.ion.ucl.ac.uk/spm; last accessed 18 December 2018). Functional time-series were realigned, coregistered to the anatomical images and normalized to F99 macaque brain template (Van Essen 2004). The time-series were band-pass filtered (0.01–0.1 Hz), nuisance corrected for ventricle and white matter signal by means of regression analysis, and motion-scrubbed for movement artefacts. A complete run was excluded when more than 25% of the frames were removed in the motion scrubbing analysis, this led to exclusion of 28 out of 327 runs (Power et al. 2012, 2014), resulting in 299 remaining runs. In other runs, the frames affected by motion were removed from the correlation analysis. More information on data acquisition and preprocessing steps can be found in the publications using this dataset (Mantini et al. 2011, 2013; Van den Heuvel et al. 2016).

For cross-model comparison with the strychnine dataset, a 3D volumetric version of the WBB47 atlas was used in which each voxel was assigned a WBB47 label. This volumetric MRI atlas was overlaid with the normalized fMRI data (Van den Heuvel, de Reus et al. 2015) and for each region an average time-series was computed by taking the mean of the time-series of all voxels within each region. Pearson correlation coefficients were calculated as a metric of rsFC between all region pairs. The individual connectivity matrices were then averaged across runs per session, then across sessions and across individuals to obtain one single group-averaged macaque functional connectivity matrix. In coherence to the collated data on strychnine neuronography, the rs-fMRI data were averaged over the 2 hemispheres to construct a single connectivity matrix as depicted in Figure 2.

Data consistency was verified by computing intra- and inter-subject variability. Intrasubject FC variability was calculated as the average correlation between all pairs of sessions of one subject ($r = 0.57$) and intersubject FC variability was calculated as the average correlation between all pairs of sessions between subjects ($r = 0.53$). Averaging FC matrices across sessions for each subject led to an average intersubject correlation ($r = 0.79$), which is comparable to human intersubject correlation ($r = 0.60$). Human FC data were adopted from 466 subjects of the Human Connectome Project (more details in Supplemental Information; Van Essen et al. 2012; Van Essen et al. 2013; Van den Heuvel, Scholtens et al. 2015).

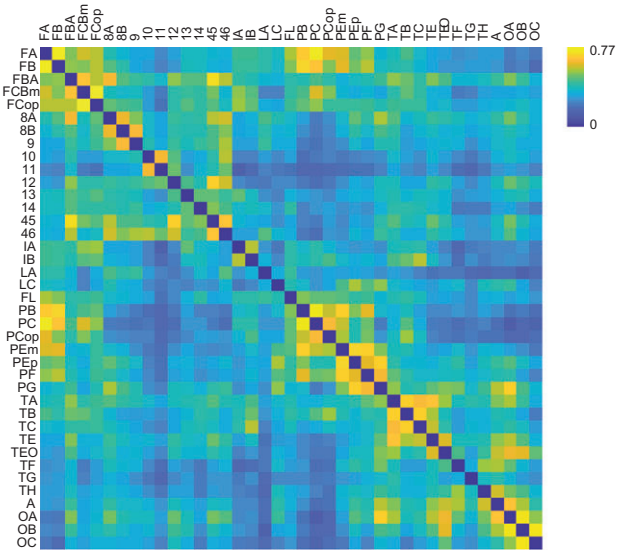

Figure 2. Resting-state functional connectivity matrix. Functional connectivity matrix of the macaque as measured by rs-fMRI. In coherence to the collated data on strychnine neuronography, the rs-fMRI data was mapped onto the WBB47 atlas and averaged over the 2 hemispheres, resulting in a group-averaged connectivity matrix (details in Methods). Color bar shows color indices for the rs-fMRI correlation values.

Main analyses were performed without global signal regression. Analyses were repeated confirming that similar findings were revealed when global signal regression was included (Murphy and Fox 2017).

Statistical Analysis

Binary Presence of Connections

The association between the presence of strychnine-based functional connections and rsFC strength was analyzed. The assignments of present ($n = 221$) and absent ($n = 428$) region pairs were based on the binary stryFC matrix. Connections indicated as "-" (i.e., unmeasured connections) were excluded from the analysis. A permutation test was used to asses statistical significance between the rsFC strength of present versus absent stryFC connections, by randomly redistributing the experimental values over 2 "random" groups (10 000 permutations). A *P*-value was assigned as the proportion of random effects exceeding the original measured difference.

Connection Strength

Jonckheere–Terpstra test was used for statistical evaluation of an ordinal structured organization of rsFC strength classified based on stryFC strength (strengths "1," "2," and "3"; $n = 51$, $n = 20$, $n = 26$, respectively; Terpstra 1952; Jonckheere 1954; Cardillo 2008). rsFC correlation values of the corresponding strength "1," "2," and "3" in the strychnine-based connectivity matrix were hypothesized to be organized as; strength "1" < strength "2" < strength "3." In the main analysis, the connections classified as present but with unknown strength ("4") were left out of the analysis. For validation, the same analysis was repeated when these connections were reclassified as the most prevalent strength in this dataset ("1," present but weak connections), or when connections were relabeled as the middle strength class ("2," present with moderate strength).

Directionality of Connections

The rsFC correlation of bidirectional ($n = 109$) and unidirectional ($n = 112$) stryFC connections was examined by means of a permutation test (10 000 permutations). Furthermore, the rsFC strength of uni- and bidirectional connections within one class of stryFC strength ("1," "2," and "3") was examined in an identical fashion (permutation test, 10 000 permutations).

Distance and Global Mean Correction

Main analyses were repeated after applying distance regression to the rsFC dataset to rule out the effect of spatial distance on the rsFC strength between cortical areas. The Euclidian distance between each region pair *i*–*j* in the WBB47 atlas was computed as the average distance between all voxels in region *i* and the voxels of region *j*. The rsFC matrix was regressed by the distance matrix, after which the residuals were used for further analysis. In addition, analyses were repeated with global mean correction.

Structural Connectivity

StryFC and rsFC were compared with anatomical tract-tracing data from the CoCoMac dataset (SC-CCM; Stephan et al. 2001; Kötter 2004) and the Markov–Kennedy dataset (SC-MK; Markov et al. 2013; Markov et al. 2014). For a description of the CoCoMac and Markov–Kennedy databases we refer to the SI. First, stryFC and rsFC strength were compared separately for absent and present connections in SC-CCM using permutation testing (10 000 permutations). Second, stryFC was examined to explain unique variance in rsFC, independent of SC-MK and distance. A multilinear model using stepwise regression with solely SC-MK as a predictor variable was used to examine whether adding stryFC to the model led to a better fit in predicting rsFC strength. Connections were included in these analyses when data was present on all modalities (stryFC, rsFC, and SC). Connections classified as present but with unknown strength ("4") in the stryFC data were only included in the analyses for which binary stryFC data was used. Two additional structure–function analyses are reported in the SI.

Results

Binary Presence of Connections

A significantly higher rsFC strength was observed for connections present in the strychnine-based connectome as compared with absent region-pairs (Fig. 3A, $P < 0.0001$, permutation test, 10 000 iterations). Similar results were obtained after controlling for distance ($P < 0.0001$), as well as when global signal regression was applied ($P < 0.0001$).

Strength of Connections

A significant ordinal organization of rsFC strength, classified based on the strength of respective stryFC connections (weak < moderate < strong), was revealed using Jonckheere–Terpstra analysis ($P < 0.01$, Fig. 3C). Similar results were obtained after controlling for distance ($P = 0.03$) and when including global signal regression ($P < 0.001$). A similar outcome was observed when connections labeled as present but with unknown strength ("4") were reassigned as connections that are present but weak ("1," $P = 0.04$) or when these connections were relabeled as present with moderate strength ("2," $P < 0.001$).

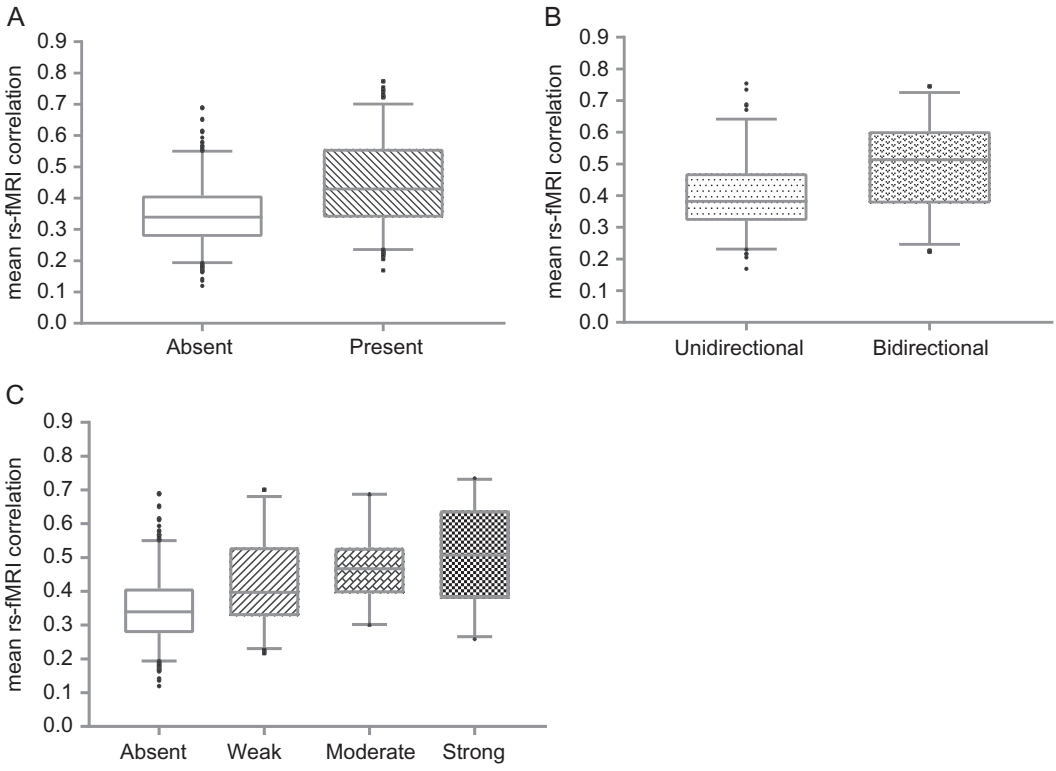

Figure 3. Evaluation of resting-state and strychnine-based functional connections of the macaque cerebral cortex. (*A*) Resting-state functional connectivity was stronger ($P < 0.0001$, 10 000 permutations) for region-pairs reported as present ($n = 221$) in strychnine-based functional connectivity as compared with absent region-pairs ($n = 428$). (*B*) Panel shows resting-state functional connectivity strength of unidirectional connections (left, $n = 109$) and bidirectional connections (right, $n = 112$) as measured by strychnine neuronography. A significant difference was observed between uni- and bidirectional connections by means of permutation testing ($P < 0.0001$, 10 000 permutations). (*C*) Relationship between resting-state functional connectivity strength and the classification of strychnine-based connection strength. Graph shows the rs-fMRI strength per group of strychnine-based strength (absent: $n = 428$; weak: $n = 51$; moderate: $n = 20$; strong: $n = 26$). A significantly ordered pattern in terms of resting-state functional connectivity strength ($P < 0.01$, weak < moderate < strong) was observed using Jonckheere Terpstra analysis. Box-and-whisker plots show the median and the second and third quartile range as the box. The whiskers represent a 90% confidence interval, observations outside this range are plotted separately.

Directionality of Connections

Region-pairs with bidirectional strychnine-based functional connections showed significantly higher rsFC strength as compared with region-pairs with unidirectional connections (Fig. 3B, $P < 0.0001$, permutation test, 10 000 iterations). Similar results were obtained after correcting for distance ($P < 0.0001$) and global mean correction ($P < 0.0001$). To rule out the possibility that significant differences between bi- and unidirectional connections might be driven by the strength of the stryFC connections, the directionality per stryFC strength class was tested. Permutation testing revealed that the bidirectional connections classified as "1" in stryFC, showed significantly higher rsFC compared with the unidirectional "1" connections ($P < 0.001$, 10 000 iterations, $n = 21$ bidirectional connections and $n = 30$ unidirectional connections; $P = 0.011$ including distance regression; $P < 0.01$ including global mean correction). No specific difference was found between bi- and unidirectional connections of strength "2" and "3" ($n = 8$ vs. $n = 12$ and $n = 6$ vs. $n = 20$, respectively). Note that only few connections were classified as "2" ($n = 20$, $P = 0.95$) and "3" ($n = 26$, $P = 0.85$), resulting in low statistical power.

Structural Connectivity

Examining a SC-FC relation, significantly higher functional connection strength was observed when a structural connection was present as compared with when no structural connection was present, for both rsFC ($P < 0.0001$) and stryFC ($P < 0.0001$). An improved model fit was observed when stryFC was added to the SC-rsFC model (explaining 2% [nonglobal mean corrected] to 5% [global mean corrected] additional variance, $P = 0.04$; nonsignificant with distance correction included, $P = 0.11$).

Discussion

Our findings substantiate the biological underpinnings of rsFC strength. Regional temporal co-activation correlation coefficients of rs-fMRI were related to data on stryFC. The presence of a physical connection facilitating strychnine-induced signal transmission was shown to correspond to a higher level of functional connectivity as measured by rs-fMRI. Higher rsFC correlations further corresponded to bidirectional connections, with unidirectional connections showing lower rsFC strength. In particular, the level of rsFC correlation between brain areas is related to the strength of underlying functional pathways.

The results of this study demonstrate the significance of variation in connection-wise rsFC correlation strength. Providing evidence that grounds this interpretation is of importance as there is ongoing discussion on how to best interpret correlation values derived from resting-state fMRI (Smith 2012). On one hand, the accuracy of rsFC networks has been suggested to be influenced by artefactual correlations due to cardiac- and

respiratory movement (Wise et al. 2004; Birn et al. 2008) and a limited spatial and temporal resolution of the cortical haemodynamic response to neuronal activity (Aguirre et al. 1998; Smith 2012). On the other hand, multiple studies point toward the direction of a functional and structural neurobiological influence on rsFC dynamics. Studies have shown that fluctuations in the BOLD signal are associated with (simultaneously recorded) local field potentials and neuronal spike rate (Shmuel et al. 2002; Logothetis 2003; Shmuel and Leopold 2008). Others have observed significant overlap between the magnitude of rs-fMRI correlations and electrophysiological recordings, substantiating the neuronal influence on rs-fMRI correlations (Nir et al. 2008). As verified in the datasets used in this study, functional resting-state connections partially reflect the structural connectivity architecture in the macaque brain (Kötter and Sommer 2000; Scholtens et al. 2014) and most resting-state patterns occur between brain regions that are both anatomically and function-wise similar (Damoiseaux et al. 2006). This study linked strychnine-based connectivity strength to rsFC strength and led to evidence of rsFC correlations to reflect biological functional connectivity between distant brain regions.

Strychnine neuronography is thought to be a well-suited measure to map the level of biological functional connectivity between different brain areas (Stephan et al. 2000). Application of strychnine creates a condition in which the stimulating effect of the source area on its target areas is increased by temporarily suppressing the GABA signaling within the source area (Shirasaki et al. 1991; Takahashi et al. 1994). Brain areas with predominantly excitatory receptor profiles and low GABA levels are associated with elevated levels of rsFC strength between cortical areas (Kapogiannis and Reiter 2012; Kapogiannis et al. 2013; Arrubla et al. 2014; Stagg et al. 2014; Bachtiar et al. 2015; Van den Heuvel et al. 2016). Therefore, strychnine application experimentally increases the functional connectivity between distant areas, enabling electrophysiological recordings of the strength of underlying functional connections. There are several considerations to be kept in mind. First it should be considered that, similar to rsFC, strychnine neuronography includes the possibility of a third region being involved in the communication between a pair of regions. Simulations of strychnine-induced activity demonstrated that monosynaptic signal transmission does not fully fit to the observed activation pattern (Frankenhaeuser 1951; Kötter and Sommer 2000), models reflecting polysynaptic signal propagation showed a significantly better fit for the strychnine-based experiments (Dusser de Barenne and McCulloch 1938; Kötter and Sommer 2000). Transmission of strychnine-based connectivity, like the correlations in resting-state fMRI, is thus likely to reflect polysynaptic coupling rather than monosynaptic signal propagation (Kötter and Sommer 2000; Stephan et al. 2000). Polysynaptic coupling being reflected by stryFC and rsFC may partly explain the moderate overlap with structural connectivity (Kötter and Sommer 2000; Lu et al. 2011; Buckner et al. 2013). Second, connections between cortical regions were included in our analyses when information was available for both stryFC and rsFC (stryFC contains 833 unmeasured connections; Stephan et al. 2000). Obtaining a complete map of stryFC would complement our analyses, but strychnine neuronography is no longer a commonly used methodology. Future studies combining observations from multiple modalities are important for gaining insight in the biological characteristics of rsFC strength and hence the interpretability of rsFC dynamics. Potential techniques to map the brain's direct functional connections may include intracranial microstimulation (Ekstrom et al. 2008) and optogenetics (Gerits and Vanduffel 2013). The development of other, noninvasive techniques, like magnetic resonance guided focused ultrasound (MRgFUS; Bystritsky et al. 2011), transcranial magnetic stimulation (TMS) or transcranial direct current stimulation (tDCS) may be appropriate in enabling translation to humans.

In conclusion, rs-fMRI functional connectivity strength is underpinned by biological features such as the presence, directionality and in particular the strength of underlying functional pathways as assessed by strychnine-based connectivity. The findings reported in this study provide an additional foundation for improved interpretation and comprehension of the biological characteristics of rs-fMRI correlation strength, which in turn may improve our understanding of often reported functional dysconnectivity effects in brain disorders.

Supplementary Material

Supplementary material is available at *Cerebral Cortex* online.

Funding

M.P.v.d.H. is an MQ fellow and was supported by an Innovational Research Incentives Scheme VIDI grant (Grant no. VIDI-452-16-015) of the Netherlands Organisation of Scientific Research (Nederlandse Organisatie voor Wetenschappelijk Onderzoek). M.P.v.d.H. and L.H.S. were supported by an ALW Open grant (Grant no. ALWOP.179) of the Netherlands Organisation of Scientific Research. L.F.B. was funded by the National Institute of Mental Health (R01 MH113234, R01 MH109464) and the National Cancer Institute (U01 CA193632). Further support came from KU Leuven Programme Financing PFV/10/008 and C14/17/109, Fonds Wetenschappelijk Onderzoek-Vlaanderen G0D5817N and G0007.12; and the European Union's Horizon 2020 Framework Programme for Research and Innovation under Grant Agreement No 720270 (Human Brain Project SGA1). Human data were provided by the Human Connectome Project, WU-Minn Consortium (Principal Investigators: David Van Essen and Kamil Ugurbil; 1U54MH091657) funded by the 16 NIH Institutes and Centers that support the NIH Blueprint for Neuroscience Research; and by the McDonnell Center for Systems Neuroscience at Washington University. The funding agencies did not have any influence on data acquisition, analysis and/or report of the data. All authors report no biomedical financial interests or potential conflicts of interest.

Notes

Conflict of Interest: None declared.

References

Aguirre GK, Zarahn E, D'Esposito M. 1998. The variability of human, BOLD hemodynamic responses. Neuroimage. 8: 360–369.

Arrubla J, Desmond H, Amkreutz C, Neuner I, Shah NJ. 2014. GABA concentration in posterior cingulate cortex predicts putamen response during resting state fMRI. PLoS One. 9: e106609.

Bachtiar V, Near J, Johansen-Berg H, Stagg CJ. 2015. Modulation of GABA and resting state functional connectivity by transcranial direct current stimulation. eLife. 4:e08789.

Bailey P, Von Bonin G, Davis EW, Garol HW, McCulloch WS, Roseman E, Silveira A. 1944. Functional organization of the medial aspect of the primate cortex. J Neurophysiol. 7:51–55.

Balan PF, Gerits A, Mantini D, Vanduffel W. 2017. Selective TMS-induced modulation of functional connectivity correlates with changes in behavior. Neuroimage. 149:361–378.

Birn RM, Smith MA, Jones TB, Bandettini PA. 2008. The respiration response function: the temporal dynamics of fMRI signal fluctuations related to changes in respiration. Neuroimage. 40:644–654.

Buckner RL, Krienen FM, Yeo BT. 2013. Opportunities and limitations of intrinsic functional connectivity MRI. Nat Neurosci. 16:832.

Buckner RL, Sepulcre J, Talukdar T, Krienen FM, Liu H, Hedden T, Andrews-Hanna JR, Sperling RA, Johnson KA. 2009. Cortical hubs revealed by intrinsic functional connectivity: mapping, assessment of stability, and relation to Alzheimer's disease. J Neurosci. 29:1860–1873.

Buckner RL, Vincent JL. 2007. Unrest at rest: default activity and spontaneous network correlations. Neuroimage. 37:1091–1096.

Bullmore E, Sporns O. 2009. Complex brain networks: graph theoretical analysis of structural and functional systems. Nat Rev Neurosci. 10:186–196.

Bystritsky A, Korb AS, Douglas PK, Cohen MS, Melega WP, Mulgaonkar AP, DeSalles A, Min BK, Yoo SS. 2011. A review of low-intensity focused ultrasound pulsation. Brain Stimul. 4:125–136.

Cardillo G. 2008. Jonckheere-Terpstra Test: A Nonparametric Test for Trend. http://www.mathworks.com/matlabcentral/fileexchange/22159 (last accessed 18 December 2018).

Chusid JG, Sugar O, French JD. 1948. Corticocortical connections of the cerebral cortex lying within the arcuate and lunate sulci of the monkey (Macaca mulatta). J Neuropathol Exp Neurol. 7:439–446.

Curtis DR, Duggan AW, Johnston GAR. 1971. The specificity of strychnine as a glycine antagonist in the mammalian spinal cord. Exp Brain Res. 12:547–565.

Damoiseaux JS, Greicius M. 2009. Greater than the sum of its parts: a review of studies combining structural connectivity and resting-state functional connectivity. Brain Struct Funct. 213:525–533.

Damoiseaux JS, Rombouts SARB, Barkhof F, Scheltens P, Stam CJ, Smith SM, Beckmann CF. 2006. Consistent resting-state networks across healthy subjects. Proc Natl Acad Sci USA. 103:13848–13853.

Davidoff RA, Aprison MH, Werman R. 1969. The effects of strychnine on the inhibition of interneurons by glycine and y-aminobutyric acid. Int J Neuropharmacol. 8:191–194.

Dusser de Barenne JG. 1916. Experimental researches on sensory localizations. Exp Physiol. 9:355–390.

Dusser de Barenne JG, McCulloch WS. 1938. Functional organization in the sensory cortex of the monkey (Macaca mulata). J Neurophysiol. 1:69–85.

Dusser de Barenne JG, McCulloch WS, Ogawa T. 1938. Functional organization in the face-subdivision of the sensory cortex of the monkey (Macaca mulatta). J Neurophysiol. 1:436–441.

Ekstrom LB, Roelfsema PR, Arsenault JT, Bonmassar G, Vanduffel W. 2008. Bottum-up dependent gating of frontal signals in early visual cortex. Science. 321:414–417.

Frankenhaeuser B. 1951. Limitations of method of strychnine neuronography. J Neurophysiol. 14:73–79.

French JD, Sugar O, Chusid JG. 1948. Corticocortical connections of the Superior Bank of the Sylvian Fissure in the monkey (Macaca mulatta). J Neurophysiol. 11:185–192.

Friston KJ. 2011. Functional and effective connectivity: a review. Brain Connect. 1:13–36.

Gerits A, Vanduffel W. 2013. Optogenetics in primates: a shining future? Trends Genet. 29:403–411.

Grayson DS, Ray S, Carpenter S, Iyer S, Costa TG, Stevens C, Nigg JT, Fair DA. 2014. Structural and functional rich club organization of the brain in children and adults. PLoS One. 9:1–13.

Greicius M. 2008. Resting-state functional connectivity in neuropsychiatric disorders. Curr Opin Neurol. 21:424–430.

Hermundstad AM, Bassett DS, Brown KS, Aminoff EM, Clewett D, Freeman S, Frithsen A, Johnson A, Tipper CM, Miller MB. 2013. Structural foundations of resting-state and task-based functional connectivity in the human brain. Proc Natl Acad Sci USA. 110:6169–6174.

Honey CJ, Sporns O, Cammoun L, Gigandet X, Thiran JP, Meuli R, Hagmann P. 2009. Predicting human resting-state functional connectivity from structural connectivity. Proc Natl Acad Sci USA. 106:2035–2040.

Jonckheere AR. 1954. A distribution-free k-sample test against ordered alternatives. Biometrika. 41:133–145.

Kapogiannis D, Reiter D. 2012. Precuneus glutamate and GABA predict default mode network activity. Neurology. 78: PD7.005.

Kapogiannis D, Reiter DA, Willette AA, Mattson MP. 2013. Posteromedial cortex glutamate and GABA predict intrinsic functional connectivity of the default mode network. Neuroimage. 64:112–119.

Keown CL, Datko MC, Chen CP, Maximo JO, Jahedi A, Müller RA. 2017. Network organization is globally atypical in autism: a graph theory study of intrinsic functional connectivity. Biol Psychiatry Cogn Neurosci Neuroimaging. 2:66–75.

Kiernan JA, Hudson AJ. 1991. Changes in sizes of cortical and lower motor neurons in amyotrophic lateral sclerosis. Brain. 114:843–853.

Kötter R. 2004. Online retrieval, processing, and visualization of primate connectivity data from the CoCoMac database. Neuroinformatics. 2:127–144.

Kötter R, Sommer FT. 2000. Global relationship between anatomical connectivity and activity propagation in the cerebral cortex. Philos Trans R Soc B Lond B Biol Sci. 355:127–134.

Logothetis NK. 2003. The underpinnings of the BOLD functional magnetic resonance imaging signal. J Neurosci. 23:3963–3971.

Lu J, Liu H, Zhang M, Wang D, Cao Y, Ma Q, Rong D, Wang X, Buckner RL, Li K. 2011. Focal pontine lesions provide evidence that intrinsic functional connectivity reflects polysynaptic anatomical pathways. J Neurosci. 31:15065–15071.

Mantini D, Corbetta M, Romani GL, Orban GA, Vanduffel W. 2013. Evolutionarily novel functional networks in the human brain? J Neurosci. 33:3259–3275.

Mantini D, Gerits A, Nelissen K, Durand JB, Joly O, Simone L, Sawamura H, Wardak C, Orban GA, Buckner RL, et al. 2011. Default mode of brain function in monkeys. J Neurosci. 31: 12954–12962.

Markov NT, Ercsey-Ravasz M, Lamy C, Gomes ARR, Magrou L, Misery P, Giroud P, Barone P, Dehay C, Toroczkai Z. 2013. The role of long-range connections on the specificity of the macaque interareal cortical network. Proc Natl Acad Sci USA. 110:5187–5192.

Markov NT, Ercsey-Ravasz MM, Ribeiro Gomes AR, Lamy C, Magrou L, Vezoli J, Misery P, Falchier A, Quilodran R, Gariel MA, et al. 2014. A weighted and directed interareal

connectivity matrix for macaque cerebral cortex. Cereb Cortex. 24:17–36.

McCulloch WS. 1944. The functional organization of the cerebral cortex. Physiol Rev. 24:390–407.

Murphy K, Fox MD. 2017. Towards a consensus regarding global signal regression for resting state functional connectivity MRI. Neuroimage. 154:169–173.

Nir Y, Mukamel R, Dinstein I, Privman E, Harel M, Fisch L, Gelbard-sagiv H, Kipervasser S, Andelman F, Neufeld MY, et al. 2008. Interhemispheric correlations of slow spontaneous neuronal fluctuations revealed in human sensory cortex. Nat Neurosci. 11:1100–1108.

Power JD, Barnes KA, Snyder AZ, Schlaggar BL, Petersen SE. 2012. Spurious but systematic correlations in functional connectivity MRI networks arise from subject motion. Neuroimage. 59:2142–2154.

Power JD, Mitra A, Laumann TO, Snyder AZ, Schlaggar BL, Petersen SE. 2014. Methods to detect, characterize, and remove motion artifact in resting state fMRI. Neuroimage. 84:320–341.

Scholtens LH, Schmidt R, de Reus MA, van den Heuvel MP. 2014. Linking macroscale graph analytical organization to microscale neuroarchitectonics in the macaque connectome. J Neurosci. 34:12192–12205.

Shirasaki T, Klee MR, Nakaye T, Akaike N. 1991. Differential blockade of bicuculline and strychnine on GABA- and glycine-induced responses in dissociated rat hippocampal pyramidal cells. Brain Res. 561:77–83.

Shmuel A, Leopold DA. 2008. Neuronal correlates of spontaneous fluctuations in fMRI signals in monkey visual cortex: implications for functional connectivity at rest. Hum Brain Mapp. 29:751–761.

Shmuel A, Yacoub E, Pfeuffer J, Van de Moortele PF, Adriany G, Hu X, Ugurbil K. 2002. Sustained negative BOLD, blood flow and oxygen consumption response and its coupling to the positive response in the human brain. Neuron. 36: 1195–1210.

Smith SM. 2012. The future of FMRI connectivity. Neuroimage. 62:1257–1266.

Stagg CJ, Bachtiar V, Amadi U, Gudberg CA, Ilie AS, Sampaio-Baptista C, O'Shea J, Woolrich M, Smith SM, Filippini N. 2014. Local GABA concentration is related to network-level resting functional connectivity. eLife. 3:e01465.

Stephan KE, Hilgetag CC, Burns GA, O'Neill MA, Young MP, Kötter R. 2000. Computational analysis of functional connectivity between areas of primate cerebral cortex. Philos Trans R Soc B Lond B Biol Sci. 355:111–126.

Stephan KE, Kamper L, Bozkurt A, Burns GAPC, Young MP, Kotter R. 2001. Advanced database methodology for the collation of connectivity data on the Macaque brain (CoCoMac). Philos Trans R Soc B Lond B Biol Sci. 356:1159–1186.

Takahashi Y, Shirasaki T, Yamanaka H, Ishibashi H, Akaike N. 1994. Physiological roles of glycine and y-aminobutyric acid in dissociated neurons of rat visual cortex. Brain Res. 640: 229–235.

Terpstra TJ. 1952. The asymptotic normality and consistency of Kendall's test against trend, when ties are present in one ranking. Indagat Math. 14:327–333.

Tian L, Jiang T, Wang Y, Zang Y, He Y, Liang M, Sui M, Cao Q, Hu S, Peng M, et al. 2006. Altered resting-state functional connectivity patterns of anterior cingulate cortex in adolescents with attention deficit hyperactivity disorder. Neurosci Lett. 400:39–43.

Van den Heuvel MP, de Reus MA, Feldman Barrett L, Scholtens LH, Coopmans FMT, Schmidt R, Preuss TM, Rilling JK, Li L. 2015. Comparison of diffusion tractography and tract-tracing measures of connectivity strength in rhesus macaque connectome. Hum Brain Mapp. 36:3064–3075.

Van den Heuvel M, Mandl R, Luigjes J, Pol HH. 2008. Microstructural organization of the cingulum tract and the level of default mode functional connectivity. J Neurosci. 28: 10844–10851.

Van den Heuvel MP, Scholtens LH, Feldman Barrett L, Hilgetag CC, de Reus MA. 2015. Bridging cytoarchitectonics and connectomics in human cerebral cortex. J Neurosci. 35:13943–13948.

Van den Heuvel MP, Scholtens LH, Turk E, Mantini D, Vanduffel W, Feldman Barrett L. 2016. Multimodal analysis of cortical chemoarchitecture and macroscale fMRI resting-state functional connectivity. Hum Brain Mapp. 37:3103–3113.

Van Essen DC. 2004. Surface-based approaches to spatial localization and registration in primate cerebral cortex. Neuroimage. 23:S97–S107.

Van Essen DC, Smith SM, Barch DM, Behrens TE, Yacoub E, Ugurbil K, Consortium W-MH. 2013. The WU-Minn human connectome project: an overview. Neuroimage. 80:62–79.

Van Essen DC, Ugurbil K, Auerbach E, Barch D, Behrens T, Bucholz R, Chang A, Chen L, Corbetta M, Curtiss SW. 2012. The Human Connectome Project: a data acquisition perspective. Neuroimage. 62:2222–2231.

Vanduffel W, Fize D, Mandeville JB, Nelissen K, Van Hecke P, Rosen BR, Tootell RBH, Orban GA. 2001. Visual motion processing investigated using contrast agent-enhanced fMRI in awake behaving monkeys. Neuron. 32:565–577.

Wise RG, Ide K, Poulin MJ, Tracey I. 2004. Resting fluctuations in arterial carbon dioxide induce significant low frequency variations in BOLD signal. Neuroimage. 21:1652–1664.

Yeo BTT, Krienen FM, Sepulcre J, Sabuncu MR, Lashkari D, Hollinshead M, Roffman JL, Smoller JW, Zöllei L, Polimeni JR, et al. 2011. The organization of the human cerebral cortex estimated by intrinsic functional connectivity. J Neurophysiol. 106:1125–1165.

Yuan M, Zhu H, Qiu C, Meng Y, Zhang Y, Shang J, Nie X, Ren Z, Gong Q, Zhang W. 2016. Group cognitive behavioral therapy modulates the resting-state functional connectivity of amygdala-related network in patients with generalized social anxiety disorder. BMC Psychiatry. 16:198.